Chapter

RGB Spectral Indices for the Analysis of Soil Protection by Vegetation Cover against Erosive Processes

Henry Antonio Pacheco Gil
and Argenis de Jesús Montilla Pacheco

Abstract

The vegetation cover plays a fundamental role in protecting the soil from erosive processes. Many researchers have developed investigations for the calculation of the RUSLE C Factor, with the use of operating bands in the near infrared. With the current advances in Geospatial Technologies, there are a good number of RGB airborne sensors in Unmanned Aerial Vehicles (UVA). The objective of this chapter is to evaluate some RGB indexes, proposed in the literature, for the protection of the soil from erosive processes by vegetation cover, in a region with a high agricultural vocation. The methodology consisted of capturing RGB images in an area of the Ecuadorian coastal region and calculating in thematic indices, within the visible one, which offer the possibility of quickly differentiating vegetation from other types of coverage on the ground. The evaluation allowed to define which indexes present the best results and adaptation to the type of crop or plant mass mapped, and to propose their use for zoning of risk of erosion under the agro-ecological conditions of the study area.

Keywords: VIgreen, UAV, risk erosion, Manabí, Ecuador, RUSLE

1. Introduction

As is well known, vegetation cover plays a fundamental role in the protection of soil from erosive processes. Recent works [1–3] have developed research for the calculation of soil erosion with the Revised Universal Soil Loss Equation (RUSLE), using multispectral information in the visible bands and infrared mainly, for the analysis of vegetation cover. Additionally, [4, 5], used multispectral images of Landsat and Sentinel satellites to evaluate vegetation cover (C FACTOR RUSLE) through image classification processes, with spatial analysis tools for GIS software. The researchers conclude that the integration of remote sensors with GIS for the assessment of vegetation cover and soil properties represent suitable methods for forecasting changes in land use and accurately and easily measuring conditions that could lead to soil loss in the future.

With the current advances in Geospatial Technologies a number of airborne sensors are available in Unmanned Aerial Vehicles (UAVs) that dramatically improve the accuracy and resolution of information. Complex algorithms where

used to detect topographical changes in agricultural surfaces with UAV images at different angles finding that vertical images are the most accurate to generate surface models that can be used in topographical evaluation, indispensable for the study of soil erosion [6]. On the other hand, the use of UAV has been reported to study the characteristics of the soil surface modified by the leveling, finding that these activities lead to a greater generation of runoff and sediment production [7].

There is a diversity of sensors for the use of UAVs in precision agriculture [8]. For the monitoring of crop and soil processes, the most commonly used sensors are those instrumented with multispectral cameras followed by thermal and hyperspectral camera and in the lastly RGB and infrared. Most works develop aerial monitoring processes that use machine learning or image processing techniques that include traditional indexes with multispectral bands.

The incorporation of multispectral sensors into UAV instruments, significantly increase costs, [9], and limit access to such technologies. For small producers with less economic resources it is proposed to use some alternative methods and indices, calculated and validated using conventional optics with visible bands [10–13]; accurate and reliable results are reported to analyze vegetation cover and its protective effect on soil. This possibility represents a strong competitive advantage for the processing of low-cost geospatial information relatively accessible to a larger number of users.

Permanent monitoring of vegetation cover is important to ensure sustainable management of agricultural activities, with a significant role in reducing water erosion. Beniaich used uncalibrated RGB images generated from a digital camera in an unmanned aerial vehicle (UAV), to assess 11 vegetation indices in the Bean and Mijo cycle study [11]. Vegetation indices with visible bands were effective tools for obtaining the soil coverage index compared to standard methods, resulting in these most practical and efficient rates in frequency and coverage area during the growing cycle.

In addition, orthomosaics in RGB have been used in multi-time periods to study physical and chemical characteristics of the soil. Better details were found for digital soil mapping, with multi-time-effective images and a classification overseen by the maximum likelihood method [5].

In summary, it shows the availability of a good variety of thematic indices within the visible range of the electromagnetic spectrum that offer the possibility of accurately and rapidly differentiating vegetation from another type of coverage on soil. For the analysis of this type of indexes it is very important to keep in mind that several of them do not respond to standardized formulas, therefore the resulting magnitudes can present a high fluctuation, and require processes of reclassification and interpretation of data according to each case.

2. Methodology

2.1 Study site

The study was developed in the experimental fields of the Faculty of Agricultural Engineering at the Universidad Tecnica de Manabí and Instituto Nacional de Investigaciones Agropecuarias (INIAP), Santa Ana town, Provinces of Manabí Ecuador (**Figure 1**). In the area of study there are different uses and soil cover, highlighting bare soils and permanent and short cycle experimental crops.

2.2 Flight platform and sensors

The aerial platform for image acquisition consisted of the UAV EBEE SQ. This SENSEFLY equipment is an advanced drone for agricultural use built around the

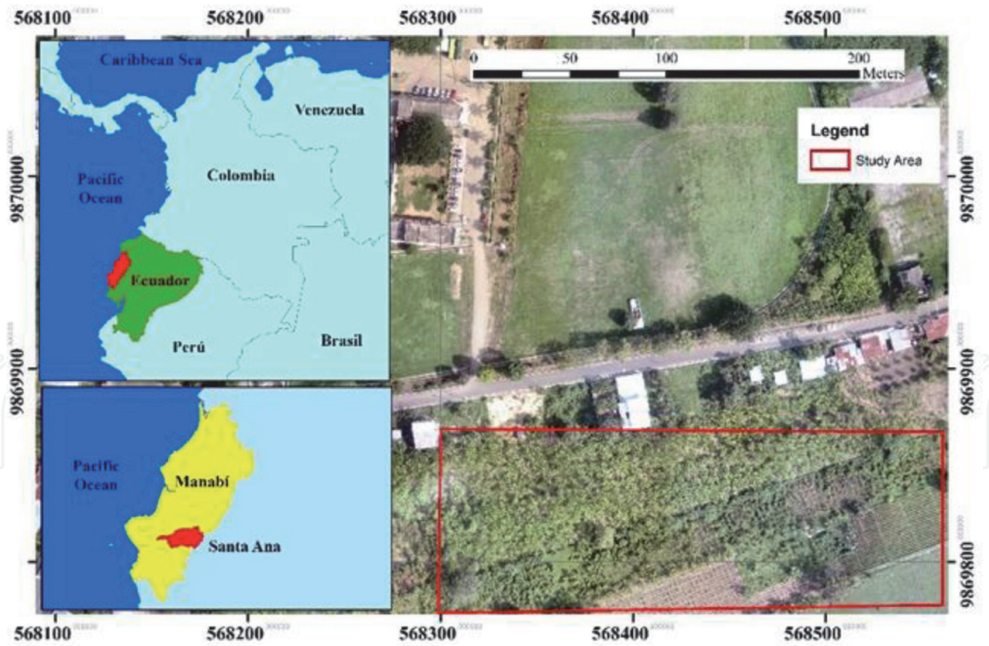

Figure 1.
Study area location.

revolutionary Parrot Sequoia camera. This multispectral sensor is a fully integrated solution in the UAV. Parrot Sequoia captures the Bands Red, Green, Red Edge (RE) and Near Infrared (NIR), and an RGB camera is also incorporated with the aim of generating an orthomosaic that supports crop analysis, as it takes the true colors of the terrain. The set is incorporated with a sunlight sensor that is located at the top of the EBEE which measures the intensity of sunlight at the time of the flight allowing normalization measurements made on different days with different light intensities, so multitemporal analyses can be performed on both cloudy and sunny days [14]. The RGB camera product was used for this research.

2.3 Imagery acquisition and processing

A photogrammetric flight was made for the acquisition of RGB images during the month of March 2020. The flight plan was programmed with the EMOTION AG software compatible with the UAV flight controller, for which the procedure specified below was fulfilled:

2.3.1 Physical inspection of the space to be flown

On the area selected for flight, the eye inspection of the space to be flown was carried out in order to identify physical elements that could cause an unwanted interruption to the flight of the drone, for example, very tall trees, antennas, sources of electromagnetism, buildings, etc. The inspection made it possible to clearly define the parameters to be considered in flight planning avoiding possible obstacles.

2.3.2 Planning the flight and photogrammetric support points

After the physical inspection the design of the flight was carried out, as well as the configuration of the shooting parameters, which are adapted to the different conditions of the flight plan, for example: the surface to be covered (which affects how quickly the photographs should be taken), flight height, transverse and

longitudinal overlaps, flight speed, the flight's daylight (which affects the camera shutter parameters), among others.

For this phase, software compatible with the drone flight controller was used, in this case it corresponds to EMOTION AG incorporated in the package at the time of the equipment purchase. It is also possible to plan with open source software available to the entire interested community.

The flight was scheduled to run autonomously, according to the parameters specified in **Table 1**.

2.3.3 Flight execution

Once the flight plan was built, it was sent to the UAV through the Emotion Ag which communicates telemetrically with the drone through its receiving antenna. After the UAV recognized the flight plan, it was executed autonomously thanks to the team's geoinformatics equipment. The conditions of the UAV during the flight were permanently monitored in real time, until the mission was completed as planned.

2.3.4 Taking photogrammetric and post-process support points

For image processing the PIX4D application was used, it can also be any other post-processing software, with which the adjustments were made and verified the quality of the images acquired to obtain the quality report. For the entry of the photogrammetric support points, 10 control points were located on the ground. On each of these points the GNSS/GPS was positioned, accurately obtaining the coordinates that were entered in the processing of the images.

For the generation of the orthomosaic and RGB bands the photographs captured by the Parrot Sequoia camera were processed with the PIX4D software, which applies radiometric corrections that allow to normalize the images and compare different photographs on the same scale taking advantage of the advantage that this program and the multispectral camera Sequoia belong to the same company, [15]. Therefore, to calculate vegetative indexes these components are the most appropriate since they incorporate specific radiometric corrections, defined in the camera parameters and software processing algorithms.

This procedure ensured a high level of accuracy in the products generated (spectral bands), as input for the calculation of spectral indices with RGB information.

Information	**Emotion AG**
Camera	Multiespectral (1.2 Mpix)+RGI
Type	Sequoia 1.7.1
Image size (cm/pixel)	11.00 cm/px
Shutter time(s)	15:47 min
Flight area	24.2 ha
Longitudinal overlap (%) 80%	80%
Transverse overlap (%) 70%	70%
Flight height (m)	150 m
Flight speed (m s^{-1})	4 m/seg

Table 1.
Parameters obtained by the Emotion AG software for flight execution.

2.4 Vegetation fraction estimation

To estimate the plant fraction above soil, nine vegetation indices were evaluated, reported in recent literature as the most appropriate in terms of results and adaptation to the type of crop or plant mass mapped. The equations and fonts for each of the selected indexes are shown in **Table 2**.

Operations for calculating indexes, according to the equations listed in **Table 2**, were performed using the Spatial Analysis tools in ArcGIS software. Specifically

Index	Equation	Reported in
Vegetation Index Green	$\mathbf{VIgreen} = \frac{Gren-Red}{Green+Red}$	Costa et al. [10] Where r, g, and b are the normalized values of the bands R (Red), G (Green), and B (Blue), respectively
Visual Atmospheric Resistance Index	$\mathbf{VARI} = \frac{Gren-Red}{Green+Red-Blue}$	
Visible NDVI	$vNDVI = 0.5268 * (r^{-0.1294} * g^{0.3389} * b^{-0.3118})$	
Index Excess Green	ExG = 2g-r-b	Beniaich et al. [11] Where r, g, and b are the normalized** values of the bands R (Red), G (Green), and B (Blue), respectively
index Excess Green Minus Excess Red	EXGR = (2g-r-b) – (1.4r – g)	
Color Index of Vegetation	CIVE = 0.441r − 0.881g + 0.385b + 18.78745	
Soil Adjusted Vegetation Index	$\mathbf{SAVI} = \frac{1.5*(Gren-Rred)}{Green+Rred+0.5}$	Beniaich et al. [11]
Modified Green Red Vegetation Index	$\boldsymbol{MGVRI} = \frac{G^2-R^2}{G^2+R^2}$	Barbosa et al. [13]
Green Leaf Index	$\mathbf{GLI} = \frac{2G-R-B}{2G+R+B}$	

** *The band values are transformed ranging from 0 to 1, according to: Marcial et al. [9]*
$\mathbf{Rn} = \frac{R}{R_{max}}\ \mathbf{Gn} = \frac{G}{G_{max}}\ \mathbf{Bn} = \frac{B}{B_{max}}$
where Rn, Gn, and Bn are the normalized values of its corresponding bands; R, G, and B are the original values of the red, green and blue, bands, respectively. Rmax = Gmax = Bmax are the maximum values for each band (255 for 24-bit colour images).
*** Obtaining the normalized spectral r, g, and b components, according to:*
$\boldsymbol{r} = \frac{Rn}{Rn+Gn+Bn}\ \boldsymbol{g} = \frac{Gn}{Rn+Gn+Bn}\ \boldsymbol{b} = \frac{Bn}{Rn+Gn+Bn}$

Table 2.
Most appropriate RGB indexes for the plant study reported in recent specialized literature.

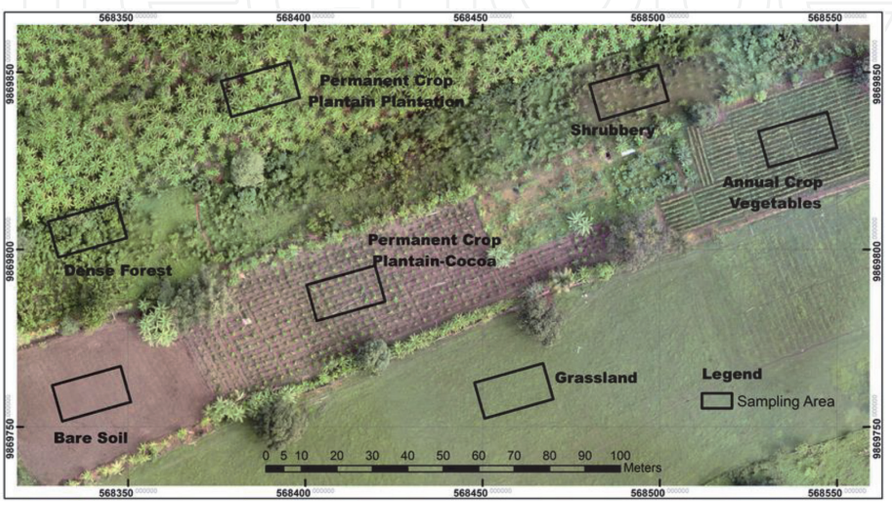

Figure 2.
Orthophoto with different coverages and selection of sampling areas.

worked on the Map Algebra tool, through which Spatial Analyst operators and functions were executed with the Raster Calculator, a simple Map Algebra expression was constructed and executed, using Python syntax in a calculator-like interface, designed for use in the application only as a tool dialog box [16].

2.5 Index evaluation according to coverage

To evaluate each of the indexes on the coverage selected in the orthophoto, **Figure 2**, a study area of 2.64 hectares was delimited with the presence of different land uses and cover. Using the principles of photointerpretation, 7 types of coverage on the area of interest were identified, which are shown in **Table 3**.

3. Analysis and results discussion

3.1 RGB image (orthophotos)

Figure 2 shows the true color composition (RGB), with excellent results in image reconstruction. Bare soil, in the southern west part of the image, is clearly differentiated, as well as early-stage crops in the central part and varied crops at different times of phenological development in the Eastern area. It stands out to the north, a banana crop in production stage with small spaces Inter crops without any protection to the soil.

The image shows very clearly the presence of a bare soil in preparation for cultivation, as well as an association of crops (banana and cocoa) in the initial state, where the development of the foliar area is still incipient and much of the soil is exposed to the watering processes. It is important to highlight that soil exposure to erosive processes, in this type of coverage should gradually decrease until very dense coverage in the medium term. It also highlights the presence of the low soil protection classes in the interplant areas of the Banana Monoculture, the alleys between the rows of the annual crop, and a specific area of fruit trees.

It is also evident specifically in areas of shrubs with the presence of tall grass and low-development trees, medium soil protection against erosive processes and a type of coverage, which represents the marginal areas of the different plant cover where good soil protection of erosive processes is initiated. This coverage is characterized by a perimeter appearance in permanent annual crops.

Good soil protection is characterized by the presence of dense vegetation and corresponds, in general, to foliar development in banana monoculture. Its expression is also very powerful in the branches of tall trees, represented in a rounded

Number	Coverage	Description
1	Null	Bare soil
2	Scarce	Permanent Crop (Plantain-Cocoa)
3	Median Low	Grassland
4	Medium dense	Annual cultivation (vegetables)
5	Dense	Shrubbery
6	Very Dense	Permanent Crop (Plantation)
7	Extremely dense	Dense forest

Table 3.
Types of coverage over the study area.

shape in the image. Likewise, they also represent this coverage in specific areas protected by small cocoa trees in the initial state of the associated crop.

There is a significant presence of two covers, with high capacity to protect the soil against erosive processes. For this particular case represented by dense forest with fruit and woodable species, as well as permanent crops in development stage and a small percentage on annual cultivation in maturity stage.

3.2 Spectral indexes

The indices obtained with RGB images were interpreted visually, grouping them into three classes (high, medium and low) according to their potential to discriminate different plant cover on the soil. **Figure 3** shows an example of each class.

Table 4 illustrates the classification of the different indexes into three categories according to their potential to discriminate covers, with different levels of soil protection before erosive processes.

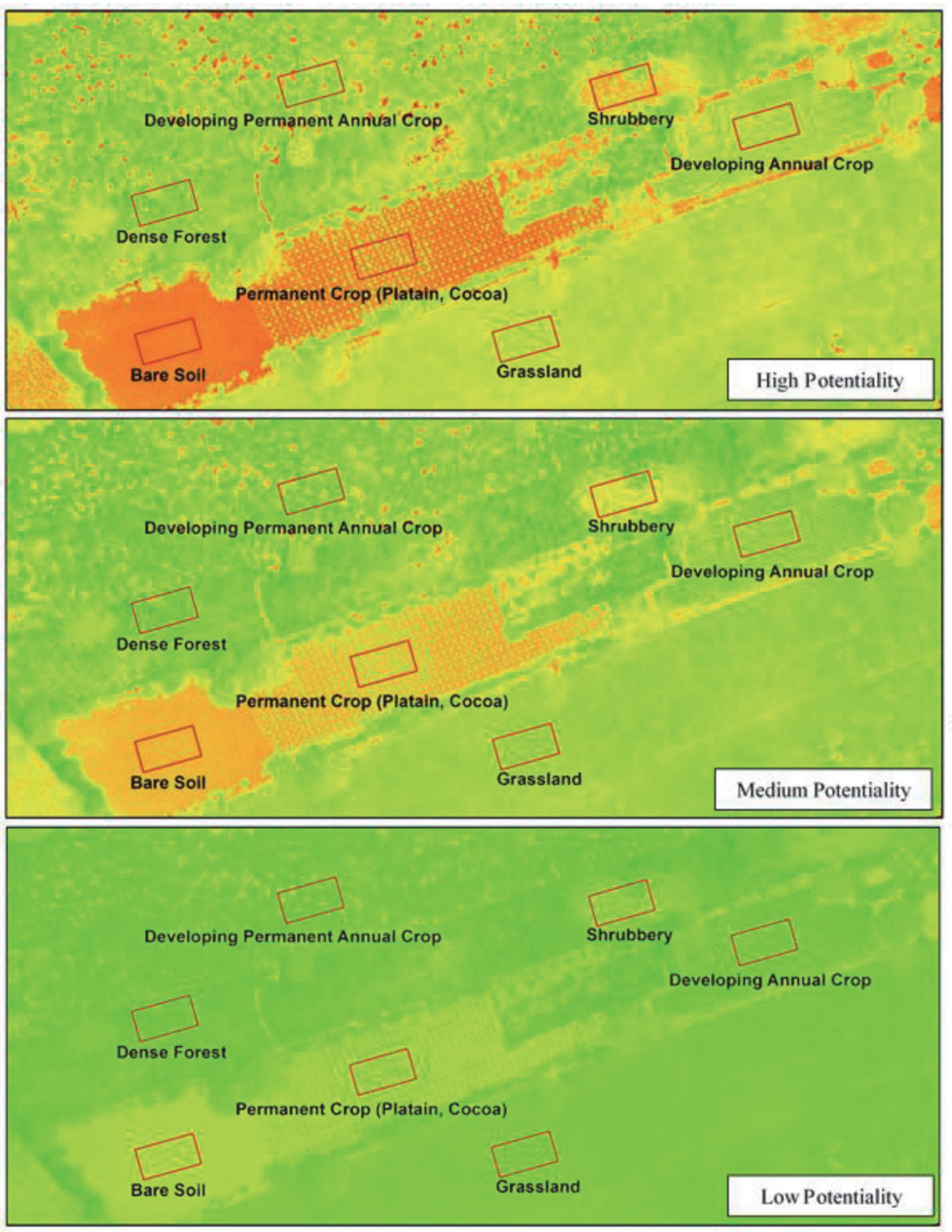

Figure 3.
Vegetation indexes with RGB data, classified according to their potential to discriminate different types of land cover.

Index	Equation	Categoría
Vegetation Index Green	$\mathbf{VIgreen} = \frac{Gren-Red}{Green+Red}$	High potentiality
Modified Green Red Vegetation Index	$\boldsymbol{MGVRI} = \frac{G^2-R^2}{G^2+R^2}$	
Index Excess Green Minus Excess Red	$\boldsymbol{EXG} = \boldsymbol{R}(2\boldsymbol{g} - \boldsymbol{r} - \boldsymbol{b}) - (1.4\boldsymbol{r} - \boldsymbol{g})$	
Index Excess Green	$\boldsymbol{ExG} = 2\boldsymbol{g} - \boldsymbol{r} - \boldsymbol{b}$	Medium potentiality
Color Index of Vegetation	$\boldsymbol{CIVE} = 0.441\boldsymbol{r} - 0.881\boldsymbol{g} + 0.385\boldsymbol{b} + 18.78745$	
Soil Adjusted Vegetation Index	$\mathbf{SAVI} = \frac{1.5*(Gren-Rred)}{Green+Rred+0.5}$	
Green Leaf Index	$\mathbf{GLI} = \frac{2G-R-B}{2G+R+B}$	
Visual Atmospheric Resistance Index	$\mathbf{VARI} = \frac{\mathbf{Gren-Red}}{\mathbf{Green+Red-Blue}}$	Low potentiality
Visible NDVI	$\boldsymbol{vNDVI} = 0.5268 * \left(\boldsymbol{r}^{-0.1294} * \boldsymbol{g}^{0.3389} * \boldsymbol{b}^{-0.3118}\right)$	

Table 4.
Classification of spectral indexes according to their potential to identify different levels of soil protection.

The Vegetation Index Green (VIgreen), was ranked first regarding its potential to discriminate different ground covers. The Modified Green Red Vegetation Index and the Excess Green Minus Excess Red Index were placed in this same category. These indexes presented very similar results and could show differences, even in an apparently homogeneous area such as bare Soil coverage. Additionally, these indices showed very good ability to differentiate unprotected soil in interplant areas in a plantain crop. In the Image, the red colors represent bare soil with little to no plant protection and therefore a high risk of erosion.

With a medium capacity to differentiate some levels of soil protection, by vegetation cover, the Soil Adjusted Vegetation Index, Index Excess Green, Color Index of Vegetation, Green Leaf Index and Index Excess Green resulted. These indexes in general tend to slightly underestimate the areas with high erosion risks, in comparison with the previous indexes, especially in covers where the density of the vegetation is lower, as is the case of annual crops and shrubs.

On the other hand, the indexes with potential slime to zoning erosive risk in soil covers were the VARI and the vNDVI, which do not manage to differentiate exactly the part of the soil discovered between the crops and practically group the different types of soils in a heterogeneous class without plant protection.

4. Conclusions

Conventional optical information, with RGB images, allowed to generate very high quality orthophotos where different levels of soil protection against erosive processes can be identified.

The coverage with the highest soil protection is offered by the forest and permanent crops while the highest erosive risk was found in the ground covers in preparation and permanent crops in the initial stage.

Three of the calculated indexes offer a high potential to discriminate covers with different levels of soil protection, being VI green the one that showed the best performance, followed by MGVRI.

Four indexes were classified as medium potential and two as low, being the VARI and the vNDVI those that occupied the last places in terms of their potential, to analyze soil protection against processes.

Author details

Henry Antonio Pacheco Gil[1*] and Argenis de Jesús Montilla Pacheco[2]

1 Facultad de Ingeniería Agrícola, Universidad Técnica de Manabí, Portoviejo, Ecuador

2 Facultad de Hotelería y Turismo, Universidad Laica Eloy Alfaro de Manabí, Ecuador

*Address all correspondence to: henry.pacheco@utm.edu.ec

References

[1] Aneseyee AB, Elias E, Soromessa T, Feyisa GL. Land use/land cover change effect on soil erosion and sediment delivery in the Winike watershed, Omo Gibe Basin, Ethiopia. Sci Total Environ [Internet]. 2020;728:138776. Available from: doi:10.1016/j.scitotenv.2020.138776

[2] Eagleston H, Marion JL. Application of airborne LiDAR and GIS in modeling trail erosion along the Appalachian Trail in New Hampshire, USA. Landsc Urban Plan [Internet]. 2020;198(August 2019): 103765. Available from: doi:10.1016/j.landurbplan.2020.103765

[3] Phinzi K, Ngetar NS. The assessment of water-borne erosion at catchment level using GIS-based RUSLE and remote sensing: A review. Int Soil Water Conserv Res. 2019;7:27–46.

[4] Jazouli A El, Barakat A, Khellouk R, Rais J, Baghdadi M El. Remote sensing and GIS techniques for prediction of land use land cover change effects on soil erosion in the high basin of the Oum Er Rbia River (Morocco). Remote Sens Appl Soc Environ [Internet]. 2019;13: 361–74. Available from: doi:10.1016/j.rsase.2018.12.004

[5] Yang H, Zhang X, Xu M, Shao S, Wang X, Liu W, et al. Hyper-temporal remote sensing data in bare soil period and terrain attributes for digital soil mapping in the Black soil regions of China. Catena [Internet]. 2020;184 (September 2019):104259. Available from: doi:10.1016/j.catena.2019.104259

[6] Meinen BU, Robinson DT. Mapping erosion and deposition in an agricultural landscape: Optimization of UAV image acquisition schemes for SfM-MVS. Remote Sens Environ [Internet]. 2020; 239(January):111666. Available from: doi:10.1016/j.rse.2020.111666

[7] Peter KD, d'Oleire-Oltmanns S, Ries JB, Marzolff I, Ait Hssaine A. Soil erosion in gully catchments affected by land-levelling measures in the Souss Basin, Morocco, analysed by rainfall simulation and UAV remote sensing data. Catena [Internet]. 2014;113:24–40. Available from: doi:10.1016/j.catena.2013.09.004

[8] Radoglou-Grammatikis P, Sarigiannidis P, Lagkas T, Moscholios I. A compilation of UAV applications for precision agriculture. Comput Networks [Internet]. 2020;172(January):107148. Available from: doi:10.1016/j.comnet.2020.107148

[9] Marcial-Pablo M de J, Gonzalez-Sanchez A, Jimenez-Jimenez SI, Ontiveros-Capurata RE, Ojeda-Bustamante W. Estimation of vegetation fraction using RGB and multispectral images from UAV. Int J Remote Sens [Internet]. 2019;40(2):420–38. Available from: doi:10.1080/01431161.2018.1528017

[10] Costa L, Nunes L, Ampatzidis Y. A new visible band index (vNDVI) for estimating NDVI values on RGB images utilizing genetic algorithms. Comput Electron Agric [Internet]. 2020;172 (March):105334. Available from: doi:10.1016/j.compag.2020.105334

[11] Beniaich A, Silva MLN, Avalos FAP, De Menezes MD, Cândido BM. Determination of vegetation cover index under different soil management systems of cover plants by using an unmanned aerial vehicle with an onboard digital photographic camera. Semin Agrar. 2019;40(1):49–66.

[12] Yeom J, Jung J, Chang A, Ashapure A, Maeda M, Maeda A, et al. Comparison of vegetation indices derived from UAV data for differentiation of tillage effects in agriculture. Remote Sens. 2019;11(13).

[13] Barbosa BDS, Ferraz GAS, Gonçalves LM, Marin DB, Maciel DT,

Ferraz PFP, et al. RGB vegetation indices applied to grass monitoring: A qualitative analysis. Agron Res. 2019;17 (2):349–57.

[14] SENSEFLY. eBeeSQ. 2020. https://www.sensefly.com/es/drone/ebee-sq/

[15] Zhou Y, Daakir M, Rupnik E, Pierrot-Deseilligny M. A two-step approach for the correction of rolling shutter distortion in UAV photogrammetry. ISPRS J Photogramm Remote Sens [Internet]. 2020;160 (November 2019):51–66. Available from: doi:10.1016/j.isprsjprs.2019.11.020

[16] ESRI. ¿Qué es el Álgebra de mapas? —ArcMap | Documentación [Internet]. 2020 [cited 2020 Sep 2]. Available from: https://desktop.arcgis.com/es/arcmap/latest/extensions/spatial-analyst/map-algebra/what-is-map-algebra.htm